



Synthesis and evaluation of 1-[2-(4-[¹¹C]methoxyphenyl)phenyl]piperazine for imaging of the serotonin 5-HT₇ receptor in the rat brain



Yoko Shimoda^a, Joji Yui^a, Lin Xie^a, Masayuki Fujinaga^a, Tomoteru Yamasaki^a, Masanao Ogawa^{a,b}, Nobuki Nengaki^{a,b}, Katsushi Kumata^a, Akiko Hatori^a, Kazunori Kawamura^a, Ming-Rong Zhang^{a,*}

^a Molecular Imaging Center, National Institute of Radiological Sciences, 4-9-1 Anagawa, Inage-ku, Chiba 263-8555, Japan

^b SHI Accelerator Service Co. Ltd., 5-9-11 Kitashinagawa, Shinagawa-ku, Tokyo 141-8686, Japan

ARTICLE INFO

Article history:

Received 24 April 2013

Revised 6 June 2013

Accepted 7 June 2013

Available online 17 June 2013

Keywords:

5-HT₇ receptor

Carbon-11

PET

Autoradiography

ABSTRACT

1-[2-(4-Methoxyphenyl)phenyl]piperazine (**4**) is a potent serotonin 5-HT₇ receptor antagonist ($K_i = 2.6$ nM) with a low binding affinity for the 5-HT_{1A} receptor ($K_i = 476$ nM). As a potential positron emission tomography (PET) radiotracer for the 5-HT₇ receptor, [¹¹C]**4** was synthesized at high radiochemical yield and specific activity, by *O*-[¹¹C]methylation of 2'-(piperazin-1-yl)-[1,1'-biphenyl]-4-ol (**6**) with [¹¹C]methyl iodide. Autoradiography revealed that [¹¹C]**4** showed in vitro specific binding with 5-HT₇ in the rat brain regions, such as the thalamus which is a region with high 5-HT₇ expression. Metabolite analysis indicated that intact [¹¹C]**4** in the brain exceeded 90% of the radioactive components at 15 min after the radiotracer injection, although two radiolabeled metabolites were found in the rat plasma. The PET study of rats showed moderated uptake of [¹¹C]**4** in the brain (1.2 SUV), but no significant regional difference in radioactivity in the brain. Pretreatment with 5-HT₇-selective antagonist SB269970 (**3**) did not decrease the uptake of [¹¹C]**4** in the rat brain. Further studies are warranted that focus on the development of PET ligand candidates with higher binding affinity for 5-HT₇ and higher in vivo stability in brain than **4**.

© 2013 Elsevier Ltd. All rights reserved.

1. Introduction

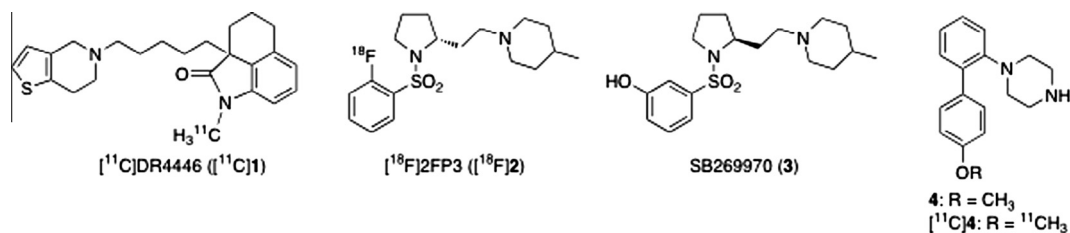
Serotonin 5-hydroxytryptamine (5-HT) receptors are classified into seven structurally and pharmacologically distinct subtypes.¹ Of these subtypes, 5-HT₇ receptor is the newest addition to the family of 5-HT receptors.^{2,3} The 5-HT₇ receptor has been cloned from the cDNA of the mouse, rat, guinea pig, and human.^{3–5} In the peripheral system of animals, stimulation of this receptor caused relaxation of the blood vessels in animals.⁶ In the central nervous system, the 5-HT₇ receptor may play roles in mediating 5-HT-induced phase shifts of neuronal activity in the suprachiasmatic nucleus of the hypothalamus.⁷ This receptor is also involved in the pathophysiology of sleep disorders, depression and schizophrenia.^{8–11} In particular, some atypical antipsychotics, such as clozapine and risperidone, showed high affinity for 5-HT₇, suggesting that the therapeutic effects of these drugs may be exerted partially via this receptor.^{12,13} The expression of 5-HT₇ mRNA is the highest in the brain, where it is discretely located within the thalamus, hypothalamus, and various limbic and cortical regions.^{3–5,14} Autoradiography has shown that the distribution pattern of 5-HT₇

in the rat and guinea pig brains is similar to the distribution pattern of mRNA in the corresponding brain regions.^{15–17}

Positron emission tomography (PET) is a useful modality for in vivo imaging and evaluation study of receptors, enzymes and plaques. In vivo visualization of the 5-HT₇ receptor would be useful to investigate its function and to elucidate its role in the pathophysiology of brain disorders. Although many potent and selective ligands for 5-HT₇ exist,^{18–21} few have been labeled for use in PET imaging studies. Ten years ago, we developed the first PET radiotracer 1-[¹¹C]methyl-2a-[4-(4,5,6,7-tetrahydrothieno[3,2-c]pyridine-5-yl)butyl]-2a,3,4,5-tetrahydro-1*H*-benz[*cd*]indole-2-one ([¹¹C]DR4446, [¹¹C]**1**; Scheme 1),²² which showed relatively high affinity for 5-HT₇ ($K_i = 9.7$ nM) and high selectivity over other 5-HT receptors.²³ A PET study using [¹¹C]**1** showed a high uptake of radioactivity (3.8 SUV) in the monkey brain and stable metabolism in the monkey plasma. However, only a low level of in vivo specific binding of [¹¹C]**1** was observed in the brain.²² Recently, 1-(2-[(2*R*)-1-[(¹⁸F]fluorophenyl)sulfonyl]pyrroline-2-yl]ethyl)-4-methylpiperidine ([¹⁸F]2FP3, [¹⁸F]**2**; $K_B = 1.43$ nM for 5-HT₇), an analog of the 5-HT₇-selective ligand SB269970 (**3**), has been developed.^{24–26} [¹⁸F]**2** is the first promising PET radiotracer to enable in vivo imaging of 5-HT₇ in the cat brain, and is likely to be a promising radiotracer for neuroimaging studies in the human brain.²⁶ However, to

* Corresponding author. Tel.: +81 43 382 3709; fax: +81 43 206 3261.

E-mail address: zhang@nirs.go.jp (M.-R. Zhang).



Scheme 1. Chemical structures of ligands for the 5-HT₇ receptor.

our knowledge, thus far, no PET radiotracer has been used for imaging and measurement studies of the 5-HT₇ receptor in the human brain.

Therefore, in this study, we developed 1-[2-(4-methoxyphenyl)phenyl]piperazine (**4**, **Scheme 1**) as a candidate of PET radiotracer for 5-HT₇. This compound showed high bind affinity to human recombinant 5-HT₇ receptors expressing in mammalian cells ($K_i = 2.6$ nM), whereas its binding affinity to 5-HT_{1A} receptor was 476 nM.^{19,27} It also displayed a weak affinity for adrenergic 1 receptor ($K_i = 156$ nM). Furthermore, compound **4** has a methoxyl group in its molecule and can be easily labeled by ¹¹C without changing its chemical structure, pharmacokinetics and pharmacological functions.

Here, we describe (1) synthesis of the unlabeled compound **4** and two novel phenol precursors **5** and **6** for radiolabeling, (2) radiosynthesis of [¹¹C]**4**, and (3) in vitro autoradiography, metabolite analysis and PET study of the rat brain for [¹¹C]**4**.

2. Results and discussion

2.1. Chemical synthesis

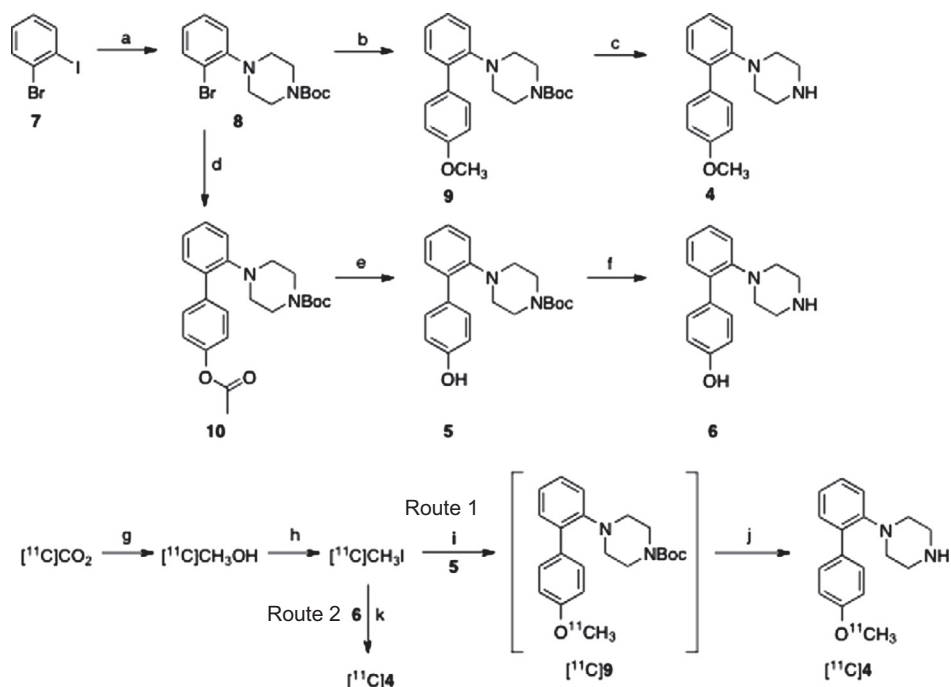
For radiolabeling, the targeted compound **4** and two precursors **5** and **6** were synthesized as shown in **Scheme 2**. Compound **4** was

prepared according to the reaction sequences reported previously with some modification.²⁷ 2-Bromo-1-iodobenzene (**7**) was treated with *tert*-butyl piperazine-1-carboxylate in the presence of Pd₂dba₃ and Xantphos to obtain *tert*-butyl 4-(2-bromophenyl)piperazine-1-carboxylate (**8**) in 46% yield. Coupling of **8** with (4-methoxyphenyl)boronic acid, followed by treatment of **9** with trifluoroacetic acid, produced **4** in 36% yield (two steps). A similar coupling reaction of **8** with 4-(4,4,5,5-tetramethyl-1,3,2-dioxaborolan-2-yl)phenyl acetate produced **10** in 59% yield, which was converted to precursor **5** by hydrolyzing **10** with NaOH. Another precursor **6** was synthesized by treating **5** with trifluoroacetic acid in 83% yield.

2.2. Radiosynthesis

[¹¹C]**4** was synthesized using a homemade automated synthesis system.²⁸ Considering the piperazine moiety in compound **4**, we first labeled **4** by reacting [¹¹C]methyl iodide ([¹¹C]CH₃I) with **5**, in which the piperazine was protected by a Boc group, followed by the deletion of the protective group in [¹¹C]**9** with trifluoroacetic acid (route 1 of **Scheme 2**).

The labeling agent [¹¹C]CH₃I was produced by reduction of cyclotron-produced [¹¹C]CO₂ with LiAlH₄, followed by iodination with 57% HI (**Scheme 2**).^{29,30} Reaction of **5** with [¹¹C]CH₃I in the



Scheme 2. Chemical synthesis and radiosynthesis: (a) *tert*-butyl piperazine-1-carboxylate, Pd₂dba₃, Xantphos, NaO(*t*-Bu), toluene, 80 °C, 16 h; (b) 4-methoxyphenylboronic acid, Pd(PPh₃)₂Cl₂, Na₂CO₃, DME–H₂O, 80 °C, 10 h; (c) trifluoroacetic acid, CH₂Cl₂, room temperature, 2 h; (d) 4-(4,4,5,5-tetramethyl-1,3,2-dioxaborolan-2-yl)phenyl acetate, Pd(PPh₃)₂Cl₂, Na₂CO₃, DME–H₂O, 80 °C, 2.5 h; (e) NaOH, H₂O–MeOH, 80 °C, 5 h; (f) trifluoroacetic acid, CH₂Cl₂, room temperature, overnight; (g) LiAlH₄, THF, –15 °C, 2 min; (h) hydroiodic acid, 180 °C, 2 min; (i) NaOH, DMF, 80 °C, 5 min; (j) trifluoroacetic acid, 100 °C, 5 min; (k) NaOH, DMF, 80 °C, 3 min.

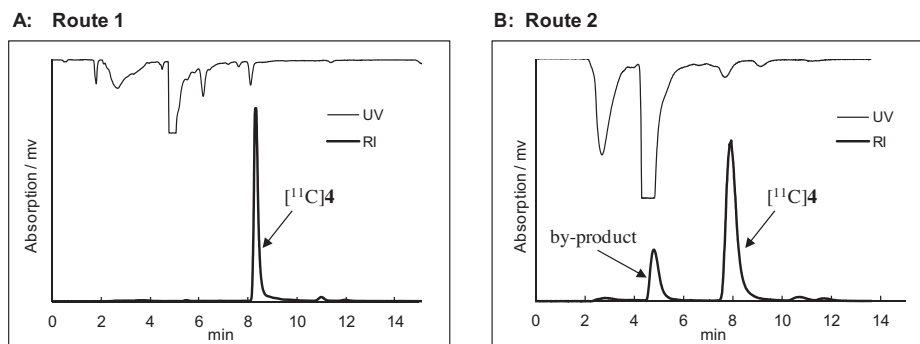


Figure 1. Chromatograms obtained on HPLC of the reaction mixtures by routes 1 (A) and 2 (B) used in the radiosynthesis of [^{11}C]4. See Section 3 for the chromatographic conditions.

presence of NaOH yielded [^{11}C]9. Without separating [^{11}C]9, the reaction mixture was treated with trifluoroacetic acid. Reverse-phase HPLC was performed to purify the reaction mixture and yield [^{11}C]4 (Fig. 1A). From 13.0 to 19.6 GBq of [^{11}C]CO₂, 1.4–2.7 GBq of [^{11}C]4 was produced in 34 ± 2 min ($n = 5$) of synthesis times from the end of bombardment (EOB), in $40 \pm 6\%$ radiochemical yield (decay-corrected, based on [^{11}C]CO₂).

Despite the high radiolabeling efficiency, it took 5 min to remove the Boc group in [^{11}C]9. More importantly, utilization of trifluoroacetic acid damaged the synthetic module. Therefore, we attempted to directly react another precursor **6** with [^{11}C]CH₃I (route 2 of Scheme 2). Without the protection of piperazine in **6**, O-[^{11}C]methylation mainly occurred on the hydroxy group, and the putative N-[^{11}C]methylated product ($t_R = 4.5$ min) was found on the HPLC separation chart as a by-product (Fig. 1B). From 7.4 to 17.0 GBq of [^{11}C]CO₂, 0.8–2.8 GBq of [^{11}C]4 was produced in $36 \pm 9\%$ radiochemical yield (decay-corrected), 54 ± 14 GBq/ μmol specific activity, >98% radiochemical purity within a synthetic time of 27 ± 2 min ($n = 3$) from EOB.

After comparing the radiolabeling efficiency, synthesis times and convenience of operating the synthetic module for the two synthetic routes, we chose to synthesize [^{11}C]4 by using route 2 for the animal experiment. At EOS, the radioactivity amount, radiochemical purity, and specific activity of [^{11}C]4 as an intravenously injectable solution were sufficient for the evaluation. The analytical results of [^{11}C]4 were in compliance with our in-house quality control/assurance specifications for radiopharmaceuticals. This product did not show radiolysis at room temperature until 100 min after formulation, indicating that [^{11}C]4 is radiochemically stable within the duration of at least one PET scan.

2.3. Computation and measurement of lipophilicity

Moderate lipophilicity is an important physicochemical property required for the development of a promising radiotracer, which facilitates high brain uptake via passage through the blood-brain barrier (BBB), without incurring nonspecific binding and for avoid-

ing problematic lipophilic brain-penetrating metabolites. The computed values of lipophilicity at pH 7.4 ($c\text{Log}D$) for **4** were 3.34. Following the labeling of **4** with ^{11}C , its lipophilicity ($\text{Log}D$) was measured using the shake flask method.³¹ The experimentally determined $\text{Log}D$ value of [^{11}C]4 was 1.67 ± 0.02 ($n = 3$). The precise reason for the difference between the $c\text{Log}D$ and $\text{Log}D$ values of [^{11}C]4 remains unclear.

2.4. In vitro autoradiography

Figure 2 shows representative in vitro autoradiography for [^{11}C]4 in the brain sections of rats ($n = 4$). In the control image (Fig. 2A), the distribution pattern of [^{11}C]4 was heterogeneous with high and moderate radioactivity in the thalamus, cerebellum, pons/medulla and striatum. Low radioactivity was observed in the hippocampus and cerebral cortex. The distribution pattern of [^{11}C]4 in the autoradiogram of brain regions was similar to the previously reported distribution pattern of 5-HT₇ receptor.^{15–17} In particular, the thalamus, which was indicated to have high 5-HT₇ density in the brain, displayed the highest radioactivity level in the brain sections. On the other hand, the hippocampus and cerebral cortex, two regions with high expression of 5-HT_{1A} receptor,³² only showed a low radioactivity, suggesting that [^{11}C]4 did not have significant specific binding for the 5-HT_{1A} receptor. This result suggested the specificity of [^{11}C]4 for 5-HT₇, which was supported by the weak binding affinity ($K_i = 476$ nM) of **4** for 5-HT_{1A}.

Incubation with unlabeled **4** at 1 μM decreased the radioactive signals in the brain sections to 60–80% of the total radioactivity in the corresponding regions of the brain (Fig. 2B). By co-incubation with the 5-HT₇-selective ligand **3**, the radioactive signals in the brain section were also reduced (Fig. 2C). The decrease in the percentage of the radioactive signals caused by **3** was similar to that caused by **4**. These results suggested that [^{11}C]4 had in vitro specific binding to 5-HT₇ in the rat brain section, although the level was not as high as the specific binding of [^{18}F]2 in the cat brain.

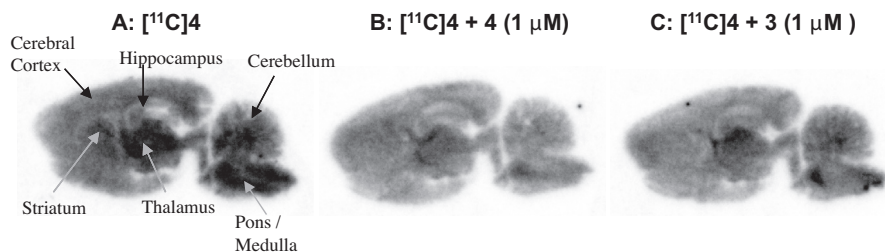


Figure 2. Representative in vitro autoradiograms of [^{11}C]4 in the brain sections. (A) [^{11}C]4 alone; (B) [^{11}C]4 with **4** (1 μM); (C) [^{11}C]4 with **3** (1 μM).

2.5. Determination of the intact form of [¹¹C]4 in rat plasma and brain

Because metabolites of a radiotracer may be present in the plasma, which may eventually enter the brain and confound the results of the PET imaging study of neuroreceptors, irrespective of whether the radiolabeled metabolites bind to the targeted neuroreceptor, we performed metabolite analysis of [¹¹C]4 in the plasma and brain of rats prior to the PET study.

The plasma and extract of homogenized brain tissues were analyzed by HPLC coupled to a highly sensitive radioactivity detector. Figure 3 shows the percentages of the intact form of [¹¹C]4 in the plasma and brain of rat at 15 and 60 min after injection. The fraction corresponding to the intact form (t_R : 7.7 min) of [¹¹C]4 in the plasma decreased to 51% at 15 min and 30% at 60 min. Two major radiolabeled metabolites (t_R : 3.3 and 5.8 min) with higher polarity than [¹¹C]4 were observed on the HPLC charts. On the other hand, unchanged [¹¹C]4 in the brain homogenate remained at 91% and 69% of the total radioactivity at 15 and 60 min, respectively. The radiolabeled metabolites in the brain showed the same retention times with the metabolites in the plasma. This result indicates that metabolism of [¹¹C]4 was relatively slow in the brain, or that only a limited level of radiolabeled metabolites originating from the plasma enter the brain. Moreover, this result suggests that the brain uptake was mainly attributed to [¹¹C]4 itself, but the radiolabeled metabolites in the brain would affect the specific binding of [¹¹C]4 to a low extent.

2.6. Small-animal PET study

Figure 4 shows representative PET images and time-activity curves in the rat brains using PET with [¹¹C]4. In the baseline measurement (Fig. 4A), [¹¹C]4 entered the rat brain rapidly after injection, and uptake of radioactivity (approximately 1.2 SUV) peaked at 3–5 min in all the regions examined, indicating that [¹¹C]4 could pass across the BBB. The uptake of radioactivity in the brain was probably relative to the lipophilicity of $\text{Log}D$ 1.67. This suggests that transporters at the BBB might not significantly limit the entrance of [¹¹C]4 into the brain. After the initial uptake, the radioactivity began to decrease in all the brain regions and was at 20–30% of the peak uptake by 90 min after the injection of [¹¹C]4. The baseline PET images showed that the radioactive signals spread throughout the brain without any significant regional differences. This distribution pattern of radioactivity was different from that observed on the *in vitro* autoradiogram. On the other hand, in the blocking experiment (Fig. 4B), pretreatment with 5-HT₇-selective **3** increased the uptake of [¹¹C]4. The radioactivity level in the examined regions was increased to approximately two-fold of that of the corresponding controls.

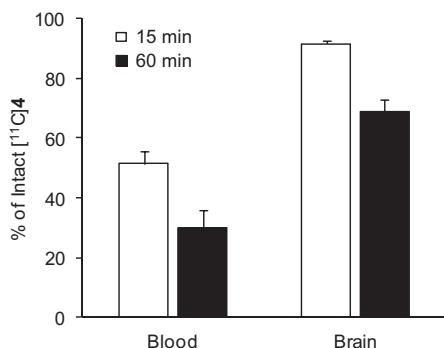


Figure 3. Metabolite analysis of [¹¹C]4 in the brain and plasma of rat ($n = 3$ in each group).

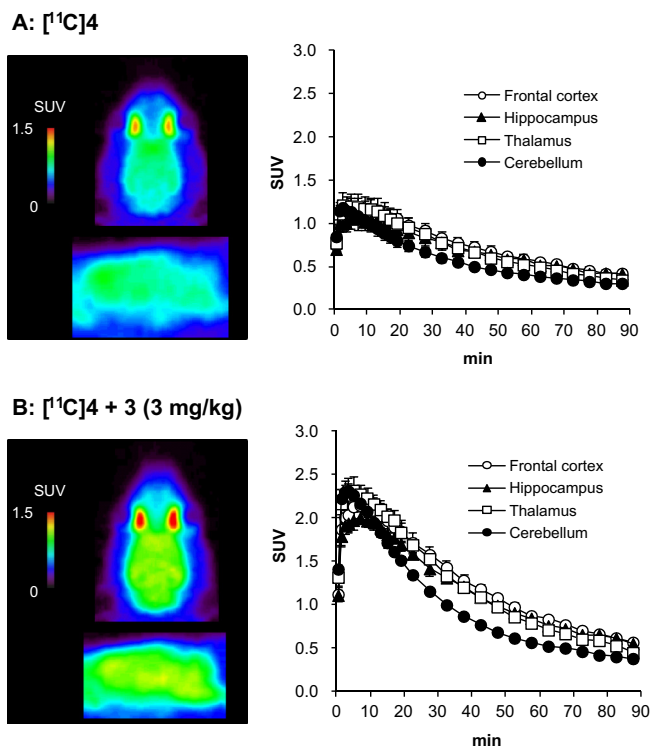


Figure 4. PET study using [¹¹C]4 in rats. Representative PET images of rat brains were showed in transverse (upper) and coronal (bottom) views. PET images were generated by summing the whole scan (0–90 min). Time-activity curves in the rat brain regions after injection of [¹¹C]4. (A) [¹¹C]4 alone; (B) [¹¹C]4 after treatment with **3** (3 mg/kg). The uptakes of radioactivity were decay-corrected to the injection time and are expressed as the standardized uptake value (SUV), normalized for the injected radioactivity and body weight. Data are the means \pm SD ($n = 3$ in each group).

The present PET study showed a relatively homogenous distribution of radioactivity in the whole brain, which was not consistent with the distribution pattern of 5-HT₇ in the brain.^{15–17} In particular, the uptake in the 5-HT₇-rich thalamus was not higher than that in the other brain regions. Moreover, the blocking experiment using 5-HT₇-selective **3** did not reduce but increased the brain uptake. Thus, it was difficult to determine whether the brain uptake was due to blood flow or due to specific binding of [¹¹C]4 in the brain based on the visual difference in PET images and kinetics between the baseline and blocking experiment. A quantification approach using brain kinetics is warranted to validate the presence of *in vivo* specific binding of [¹¹C]4 to 5-HT₇ in the brain. To this end, arterial input measures in rat using quantitative analysis method, such as Lassen graphic analysis, should be performed.

Taken together, although [¹¹C]4 exhibited *in vitro* binding with 5-HT₇, moderate brain uptake and relatively stable metabolism in the brain, *in vivo* evaluation showed limited specificity of [¹¹C]4 for 5-HT₇. The level of specific binding in the brain appeared to be lower than that of [¹⁸F]2, the most promising radiotracer for 5-HT₇ to date. Therefore, further studies should be conducted that focus on the development of ligand candidates with more potent binding affinity for 5-HT₇ than that of **4**.

In general, the ratio of density (B_{max}) of a targeted receptor in the brain tissues to the equilibrium dissociation constant (K_D) of a radiotracer is used to predict the magnitude of specific binding in a PET imaging study. The ratio of B_{max}/K_D , also indicated as binding potential, should preferably be >2 to elucidate specific binding on the basis of individual experiences.³³ Although no data regarding the B_{max} of 5-HT₇ have been reported, the density of the 5-HT₇ receptor was determined to be less than one-tenth of that of the

other 5-HT₇ subtypes.³⁴ The 5-HT_{1A} B_{\max} , for example, was measured to be 5–10 nM in the hippocampus and frontal cortex of the rat brain,³⁵ therefore, the B_{\max} of 5-HT₇ in the brain could be assumed to be 0.5–1 nM. Considering the ratio of B_{\max}/K_D , the binding affinity of **4** ($K_i = 2.6$ nM) may be not sufficient to elucidate in vivo specific binding to the 5-HT₇ receptor in the brain. Therefore, to visualize this receptor in the brain, novel candidates for PET tracers with higher binding affinity for 5-HT₇ and high in vivo stability in brain than **4** are required. Consequently, new compounds are being designed, with modified chemical structures for the optimization of a PET radiotracer.

In conclusion, this study describes the synthesis and evaluation of [¹¹C]**4** as a potential PET radiotracer for the imaging of the 5-HT₇ receptor in the rat brain. [¹¹C]**4** was synthesized by *O*-[¹¹C]methylation of the desmethyl precursor **6** with [¹¹C]CH₃I, producing a high radiochemical yield and specific activity. Although [¹¹C]**4** showed in vitro specific binding in the brain, the present evaluation could not show the presence of in vivo specific binding of [¹¹C]**4** to the 5-HT₇ receptor. Further optimization of the structure of [¹¹C]**4** will thus be required to achieve in vivo imaging of the 5-HT₇ receptor in the brain.

3. Experimental section

Melting points (mp) were uncorrected in this study. ¹H NMR spectra were recorded on a JNM-AL-300 spectrometer (JEOL; Tokyo, Japan) using tetramethylsilane as an internal standard. All chemical shifts (δ) were reported in parts per million (ppm) downfield from the standard. High resolution (HR) fast atom bombardment-mass spectrometry (FAB-MS) was performed using JEOL NMS-SX102 spectrometer (JEOL). Column chromatography was performed on Wakogel C-200 (Wako Pure Chemical Industries, Ltd.; Osaka, Japan). HPLC was performed using a JASCO HPLC system (JASCO; Tokyo, Japan): effluent radioactivity was monitored using a NaI (TI) scintillation detector system. SB269970 (**3**) was purchased from ALEXIS BIOCHEMICALS (San Diego, CA). All chemical reagents of the highest grade commercially available were purchased from Sigma–Aldrich Corporation (Milwaukee, WI) or Wako Pure Chemical Industries, Ltd. or Tokyo Chemical Industries, Ltd. (Tokyo, Japan). ¹¹C was produced using a CYPRIS HM-18 cyclotron (Sumitomo Heavy Industry; Tokyo, Japan). Unless otherwise stated, radioactivity was measured using an IGC-3R Curiometer (Hitachi Aloka Medical, Ltd., Tokyo, Japan). All animal experiments were performed according to the recommendations of the Committee for the Care and Use of Laboratory Animals, National Institute of Radiological Sciences (Chiba, Japan). Animals were maintained and handled in accordance with the recommendations of the National Institute of Health and the institutional guidelines of the National Institute of Radiological Sciences. Sprague–Dawley male rats (220–240 g, 7 weeks) were provided by Japan SLC (Shizuoka, Japan).

3.1. Chemical synthesis

3.1.1. *tert*-Butyl 4-(2-bromophenyl)piperazine-1-carboxylate (**8**)

A mixture of 1-bromo-2-iodobenzene (**7**; 626 μ L, 5.08 mmol), *tert*-butyl piperazine-1-carboxylate (942 mg, 5.06 mmol), NaO (*t*-Bu) (739 mg, 7.69 mmol), Xantphos (292 mg, 10 mol %) and Pd₂dba₃ (115 mg, 5 mol % Pd) in toluene (14 mL) was heated at 80 °C for 16 h under N₂ gas. The reaction mixture was poured into water and extracted with CH₂Cl₂. The organic layer was washed with brine, dried over anhydrous Na₂SO₄ and concentrated under reduced pressure. Purification of the residue by silica gel column chromatography (EtOAc/*n*-hexane, 1/10, v/v) yielded **8** (786 mg, 46%) as a pale yellow oil. ¹H NMR (300 MHz, CDCl₃): δ 1.49 (9H,

s), 2.98 (4H, t, $J = 4.8$ Hz), 3.61 (4H, t, $J = 4.8$ Hz), 6.90–6.96 (1H, m), 7.02 (1H, dd, $J = 1.6, 8.1$ Hz), 7.25–7.30 (1H, m), 7.57 (1H, d, $J = 7.9$ Hz). ¹³C NMR (75 MHz, CDCl₃): δ 28.4, 43.9 (br), 51.6, 79.8, 120.0, 121.0, 124.7, 128.3, 133.9, 150.4, 154.9. FAB-MS: m/z 341 (M+H).

3.1.2. *tert*-Butyl 2-[(4-methoxyphenyl)phenyl]piperazine-1-carboxylate (**9**)

A mixture of **8** (252 mg, 0.74 mmol), 4-methoxyphenylboronic acid (136 mg, 0.89 mmol), Na₂CO₃ (239 mg, 2.25 mmol) and Pd(PPh₃)₂Cl₂ (17 mg, 3 mol % Pd) in dimethyl ether (DME)/water (8 mL, 3/1, v/v) was heated at 80 °C for 10 h under N₂ gas. The reaction mixture was poured into water and extracted with ether. The organic layer was washed with brine, dried over anhydrous Na₂SO₄ and concentrated under reduced pressure. Purification of the residue by silica gel column chromatography (EtOAc/*n*-hexane, 1/10, v/v) yielded **9** (191 mg, 70%) as a colorless crystal; mp, 153–155 °C. ¹H NMR (300 MHz, CDCl₃): δ 1.44 (9H, s), 2.78 (4H, br), 3.32 (4H, br), 3.85 (3H, s), 6.93 (2H, d, $J = 8.4$ Hz), 6.99 (1H, d, $J = 7.5$ Hz), 7.08–7.10 (1H, m), 7.22–7.26 (2H, m), 7.57 (2H, d, $J = 7.5$ Hz). ¹³C NMR (75 MHz, CDCl₃): δ 28.4, 43.1 (br), 50.9, 55.2, 79.6, 113.6, 118.4, 123.1, 127.9, 129.9, 131.4, 133.2, 134.9, 150.0, 154.9, 158.5. FAB-MS: m/z 369 (M+H).

3.1.3. 1-[2-(4-Methoxyphenyl)phenyl]piperazine (**4**)

A mixture of **9** (104 mg, 0.30 mmol) and trifluoroacetic acid (460 μ L, 5.97 mmol) in CH₂Cl₂ (3 mL) was stirred at room temperature for 2 h. The reaction mixture was poured into saturated aqueous NaHCO₃ and extracted with CH₂Cl₂. The organic layer was washed with brine, dried over anhydrous Na₂SO₄ and concentrated under reduced pressure to obtain **4** (43 mg, 52%) as a pale yellow oil. ¹H NMR (300 MHz, CDCl₃): δ 1.68 (1H, br, D₂O exchanged), 2.78 (8H, s), 3.85 (3H, s), 6.94 (2H, d, $J = 8.4$ Hz), 7.03–7.08 (2H, m), 7.21–7.29 (2H, m), 7.59 (2H, d, $J = 8.4$ Hz). ¹³C NMR (75 MHz, CDCl₃): δ 46.1, 52.4, 55.2, 113.5, 118.3, 122.6, 127.9, 129.9, 131.3, 133.5, 134.7, 150.7, 158.4. HRMS (FAB) calcd for C₁₇H₂₁ON₂, 269.1654; found, 269.1640.

3.1.4. *tert*-Butyl 2-[(4-acetoxyphenyl)phenyl]piperazine-1-carboxylate (**10**)

A mixture of **8** (282 mg, 0.83 mmol), 4-(4,4,5,5-tetramethyl-1,3,2-dioxaborolan-2-yl)phenyl acetate (260 mg, 0.99 mmol), Na₂CO₃ (261 mg, 2.46 mmol) and Pd(PPh₃)₂Cl₂ (18 mg, 3 mol % Pd) in DME/water (8 mL, 3/1, v/v) was heated at 80 °C for 2.5 h under N₂ gas. The reaction mixture was poured into saturated aqueous NaHCO₃ and extracted with ether. The organic layer was washed with brine, dried over anhydrous Na₂SO₄ and concentrated under reduced pressure. Purification of the residue by silica gel column chromatography (EtOAc/*n*-hexane, 1/10, v/v) yielded **10** (193 mg, 59%) as a colorless crystal; mp, 123–124 °C. ¹H NMR (300 MHz, CDCl₃): δ 1.43 (9H, s), 2.31 (3H, s), 2.77 (4H, br), 3.31 (4H, br), 7.01 (1H, d, $J = 7.7$ Hz), 7.06–7.16 (3H, m), 7.23–7.31 (2H, m), 7.63 (2H, d, $J = 8.4$ Hz). ¹³C NMR (75 MHz, CDCl₃): δ 21.2, 28.4, 44.1 (br), 51.2, 79.7, 118.7, 121.3, 123.4, 128.6, 129.9, 131.5, 134.4, 138.3, 149.6, 149.7, 154.8, 169.5. FAB-MS: m/z 397 (M+H).

3.1.5. *tert*-Butyl 2-[(4-hydroxyphenyl)phenyl]piperazine-1-carboxylate (**5**)

A mixture of **8** (190 mg, 0.49 mmol) and aqueous 1 M NaOH (1 mL) in MeOH/water (7 mL, 6/1, v/v) was heated at 80 °C for 5 h. After cooling to room temperature, MeOH was removed under reduced pressure. The reaction mixture was adjusted to pH 7 with aqueous 0.1 M HCl, and extracted with CH₂Cl₂. The organic layer was washed with saturated aqueous NaHCO₃, dried over anhydrous Na₂SO₄ and concentrated under reduced pressure to obtain **5** (137 mg, 80%) as a colorless crystal; mp, 208–209 °C. ¹H NMR

(300 MHz, CDCl₃): δ 1.38 (9H, s), 2.69 (4H, br), 3.23 (4H, br), 6.80 (2H, d, J = 8.4 Hz), 6.99–7.07 (2H, m), 7.14–7.22 (2H, m), 7.45 (2H, d, J = 8.4 Hz), 9.43 (1H, s). ¹³C NMR (75 MHz, CDCl₃): δ 28.4, 44.0 (br), 50.8 (br), 80.0, 115.1, 118.3, 123.0, 127.9, 130.1, 131.3, 132.9, 134.9, 150.0, 155.0, 155.1. HRMS (FAB) calcd for C₂₁H₂₇O₃N₂, 355.2022; found, 355.2041.

3.1.6. 1-[2-(4-Hydroxyphenyl)phenyl]piperazine (6)

A mixture of compound **5** (99 mg, 0.28 mmol) and trifluoroacetic acid (862 μ L, 11.2 mmol) was stirred overnight at room temperature. After removal of trifluoroacetic acid under reduced pressure, purification of the residue by silica gel column chromatography (EtOAc/MeOH/Et₃N, 9/1/0.001, v/v/v) to give trifluoroacetate of **6** (85 mg, 83%) as a pale pink crystal; mp, 177–179 °C. ¹H NMR (300 MHz, DMSO-*d*₆): δ 2.93 (4H, s), 3.01 (4H, s), 6.82 (2H, d, J = 8.4 Hz), 7.02–7.10 (2H, m), 7.16–7.27 (2H, m), 7.44 (2H, d, J = 8.4 Hz), 8.88 (2H, br), 9.58 (1H, br). ¹³C NMR (75 MHz, DMSO-*d*₆): δ 43.0, 47.4, 115.3, 118.4, 123.4, 127.8, 129.4, 130.5, 130.9, 134.2, 148.6, 156.5. HRMS (FAB) calcd for C₁₆H₁₉ON₂, 255.1497; found, 255.1485.

3.2. Radiosynthesis of 1-[2-(4-[¹¹C]methoxyphenyl)phenyl]piperazine ([¹¹C]**4**)

3.2.1. Route 1

After irradiation, the cyclotron-produced [¹¹C]CO₂ was bubbled into 0.4 M LiAlH₄ in anhydrous THF (300 μ L). After evaporation of THF, the remaining complex was treated with 57% HI (300 μ L) to produce [¹¹C]CH₃I, which was distilled and transferred under N₂ gas flow into a solution of **5** (1.0 mg) and NaOH (6 μ L, 0.5 M) in anhydrous DMF (100 μ L) at –15 to –20 °C. When the radioactivity reached a plateau, the reaction mixture was subsequently heated at 80 °C for 5 min. After [¹¹C]methylation, trifluoroacetic acid (200 μ L) was added and this resulting solution was heated at 100 °C for another 5 min. After adding NaOAc (1.5 mL, 2.5 M), the final mixture was subjected to HPLC. HPLC separation was completed on a Capcell Pak C₁₈ column (10 mm id \times 250 mm; Shiseido, Tokyo, Japan) using MeCN/H₂O/trifluoroacetic acid (4/6/0.05, v/v/v) at 5.0 mL/min. The radioactive fraction corresponding to [¹¹C]**4** (t_R : 8.8 min) was collected in a sterile flask, evaporated to dryness under reduced pressure, redissolved in 3 mL of sterile normal saline, and passed through a 0.22 μ m Millipore filter to obtain 2.7 GBq of [¹¹C]**4**.

The radiochemical purity of [¹¹C]**4** (t_R : 7.8 min) was analyzed using HPLC with a detector for monitoring radioactivity under the following conditions: Capcell Pak C₁₈ column, 4.6 mm id \times 250 mm; MeCN/H₂O/trifluoroacetic acid (4/6/0.05, v/v/v), 1.0 mL/min. The identity of [¹¹C]**4** was confirmed by HPLC analysis with unlabeled **4**. The specific activity was calculated by comparing the assayed radioactivity to the mass measured at UV 254 nm. The synthesis time was 35 min from EOB; radiochemical yield (decay-corrected): 46% based on [¹¹C]CO₂; radiochemical purity: >99%; and specific activity at EOS: 100 GBq/ μ mol.

3.2.2. Route 2

[¹¹C]CH₃I was produced and transferred into anhydrous DMF (300 μ L) containing **6** (0.8 mg) and NaOH (10 μ L, 0.5 M) at –15 to –20 °C. This reaction mixture was heated to 80 °C and maintained for 3 min. After MeCN/H₂O/trifluoroacetic acid (1 mL, 4/6/0.05, v/v/v) was added to the reaction vessel, the radioactive mixture was transferred into a reservoir for HPLC purification (Capcell Pak C₁₈ column, 10 mm id \times 250 mm; MeCN/H₂O/trifluoroacetic acid = 4/6/0.05, 5 mL/min). The desired radioactive fraction was treated as described above to obtain [¹¹C]**4** (1.84 GBq at EOS) as an injectable solution. The synthesis time was 29 min from EOB; radiochemical yield (decay-corrected): 45% based on [¹¹C]CO₂;

radiochemical purity: >99%; and specific activity at EOS: 55 GBq/ μ mol.

3.3. Measurement of partition co-efficients (Log *D*)

Partition co-efficient values were measured by mixing [¹¹C]**4** (radiochemical purity: 100%; approximately 150,000 cpm) with *n*-octanol (3.0 g) and sodium phosphate-buffered saline (PBS, 3.0 g; 0.1 M, pH 7.40) in a test tube. The tube was vortexed for 3 min at room temperature, followed by centrifugation at 3500 rpm for 5 min. An aliquot of 1 mL PBS and 1 mL *n*-octanol was removed, weighted, and counted. Samples from the remaining organic layer were removed and re-partitioned until consistent Log*D* values were obtained. The Log*D* value was calculated by comparing the ratio of cpm/g of *n*-octanol to that of PBS and expressed as Log*D* = Log[cpm/g (*n*-octanol)/cpm/g(PBS)]. All assays were performed in triplicate. Meanwhile, the value of *c*Log*D* of [¹¹C]**4** was computed using Pallas 3.4 software (CompuDrug; Sedona, AZ).

3.4. In vitro autoradiography

Four rat brains were quickly removed and frozen on powdered dry ice. Sagittal sections (20 μ m) of the brain were cut using a cryostat microtome (HM560; Carl Zeiss, Germany) and thaw-mounted on glass slides, which were then dried and stored at –80 °C until use. Brain sections were preincubated (3 \times 5 min) in Tris–HCl (50 mM, pH 7.4) at room temperature. After preincubation, these sections were incubated for 30 min at room temperature in fresh buffer with [¹¹C]**4** (1 nM, 37 MBq/200 mL). Unlabeled **4** or **3** (1 μ M) was used to elucidate the specific binding of [¹¹C]**4** for 5-HT₇. After incubation, the sections were washed (3 \times 5 min) with cold buffer, dipped in cold distilled water, and dried with cold air. These sections were placed in contact with imaging plates (BAS-MS2025; FUJIFILM, Tokyo, Japan). Autoradiograms were obtained and photo-stimulated luminescence values (PSL) in the regions of interest (ROIs) were measured using a Bio-Imaging Analyzer System (BAS5000, FUJIFILM).

3.5. Metabolite assay for rat plasma and brain homogenate

The rat brain was dissected and the brain sections were homogenized in an ice-cooled MeCN/H₂O (1:1, 1.0 mL) solution, respectively. The homogenate was centrifuged at 15,000 rpm for 2 min at 4 °C and the supernatant was collected. The recovery of radioactivity into the supernatant was 68–87% based on the total radioactivity in the brain homogenate.

An aliquot of the supernatant (100–500 μ L) obtained from the plasma or brain homogenate was injected into the radio-HPLC system, and analyzed under the same analytical conditions described above. The percentage of [¹¹C]**4** to total radioactivity (corrected for decay) on the HPLC charts was calculated as (peak area for [¹¹C]**4**/total peak area) \times 100.

3.6. PET imaging

PET scans were performed using a small-animal Inveon PET scanner (Siemens Medical Solutions USA, Knoxville, TN), which provides 0.796 mm (center-to-center)-apart 159 transaxial slices, 10 cm transaxial FOV, and 12.7 cm axial FOV. Before the scans, the rats were anesthetized with 5% (v/v) isoflurane, and maintained thereafter with 1–2% (v/v) isoflurane. Emission scans were acquired for 90 min in a 3-dimensional list mode with an energy window of 350–750 keV, immediately after an intravenous injection of [¹¹C]**4** (16–18 MBq/200 μ L, 0.07–0.11 nmol). To evaluate in vivo specific binding, unlabeled **3** (3 mg/kg dissolved in 300 μ L

saline containing 10% ethanol and 5% polysorbate 80) was injected 1 min before injection of [¹¹C]4. Three rats were used for each experiment. All list-mode acquisition data were sorted into 3-dimensional sinograms, which were then Fourier rebinned into 2-dimensional sinograms (frames × min: 4 × 1, 8 × 2, 14 × 5). Dynamic images were reconstructed with filtered back-projection using a Hanning's filter, with a Nyquist cutoff of 0.5 cycle/pixel. ROIs were placed on the striatum, hippocampus, cerebral cortex, thalamus, medulla, and cerebellum using ASIPro VM™ (Analysis Tools and System Setup/Diagnostics Tool, Siemens Medical Solutions, USA) with reference to the MRI template. The uptake of radioactivity in the brain was decay-corrected to the injection time and was expressed as the standardized uptake value (SUV), which was normalized to the injected radioactivity and body weight. SUV = (radioactivity per milliliter tissue/injected radioactivity) × gram body weight.

Acknowledgments

We thank the crew of the Cyclotron Operation Section and Molecular Imaging Center of National Institute of Radiological Sciences for their help with the operation of the cyclotron, production of the radioisotope and animal experiments.

References and notes

- Matthes, H.; Boschert, U.; Amlaiky, N.; Grailhe, R.; Plassat, J. L.; Muscatelli, F.; Mattei, M. G.; Hen, R. *Mol. Pharmacol.* **1993**, *43*, 313.
- Eglen, R. M.; Jasper, J. R.; Chang, D. J.; Martin, G. R. *Trends Pharmacol. Sci.* **1997**, *18*, 104.
- Shen, Y.; Monsma, F. J., Jr.; Metcalf, M. A.; Jose, P. A.; Hamblin, M. W.; Sibley, D. R. *J. Biol. Chem.* **1993**, *268*, 18200.
- Tsou, A. P.; Kosaka, A.; Bach, C.; Zuppan, P.; Yee, C.; Tom, L.; Alvarez, R.; Ramsey, S.; Bonhaus, D. W.; Stefanich, E.; Jakeman, L.; Eglén, R. M.; Chan, H. W. *J. Neurochem.* **1994**, *63*, 456.
- Bard, J. A.; Zgombick, J.; Adham, N.; Vaysse, P.; Brancheck, T. A.; Weinshank, R. L. *J. Biol. Chem.* **1994**, *268*, 23422.
- Cushing, D. J.; Zgombick, J. M.; Nelson, D. L.; Cohen, M. L. *J. Pharmacol. Exp. Ther.* **1996**, *277*, 1560.
- Sleight, A. J.; Carolo, C.; Petit, N.; Zwingelstein, C.; Bourson, A. *Mol. Pharmacol.* **1995**, *47*, 99.
- Vanhoenacker, P.; Haegeman, G.; Leysen, J. E. *Trends Pharmacol. Sci.* **2000**, *21*, 70.
- Abbas, A. I.; Hedlund, P. B.; Huang, X. P.; Tran, T. B.; Meltzer, H. Y.; Roth, B. L. *Psychopharmacology* **2009**, *206*, 119.
- Hedlund, P. B.; Sutcliffe, J. G. *Trends Pharmacol. Sci.* **2004**, *25*, 481.
- Mnie-Filali, O.; Lambas-Señas, L.; Scarna, H.; Haddjeri, N. *Curr. Drug Targets* **2009**, *10*, 1109.
- Roth, B. L.; Craigo, S. C.; Choudhary, M. S.; Ulver, A.; Monsma, F. J., Jr.; Shen, Y.; Meltzer, H. Y.; Sibley, D. R. *J. Pharmacol. Exp. Ther.* **1994**, *268*, 1403.
- Cates, L. N.; Roberts, A. J.; Huitron-Resendiz, S.; Hedlund, P. B. *Neuropharmacology* **2013**, *70C*, 211.
- Kinsey, A. M.; Wainwright, A.; Heavens, R.; Sirinathsinghji, D. J.; Oliver, K. R. *Brain Res. Mol. Brain Res.* **2001**, *88*, 194.
- Ruat, M.; Traffort, E.; Leurs, R.; Tardivel-Lacombe, J.; Diaz, J.; Arrang, L. M.; Schwartz, J. C. *Proc. Natl. Acad. Sci. U.S.A.* **1993**, *90*, 8547.
- To, Z. P.; Bonhaus, D. W.; Eglén, R. M.; Jakeman, L. B. *Br. J. Pharmacol.* **1995**, *115*, 107.
- Gustafan, E. L.; Durkin, M. M.; Bard, J. A.; Zgombick, J.; Brancheck, T. A. *Br. J. Pharmacol.* **1996**, *117*, 657.
- Pittalà, V.; Salerno, L.; Modica, M.; Siracusa, M. A.; Romeo, G. *Mini. Rev. Med. Chem.* **2007**, *7*, 945.
- Leopoldo, M.; Lacivita, E.; Berardi, F.; Perrone, R.; Hedlund, P. B. *Pharmacol. Ther.* **2011**, *129*, 120.
- Pittalà, V.; Pittalà, D. *Mini. Rev. Med. Chem.* **2011**, *11*, 1108.
- Kim, Y.; Kim, J.; Tae, J.; Roth, B. L.; Rhim, H.; Keum, G.; Nam, G.; Choo, H. *Bioorg. Med. Chem.* **2013**. <http://dx.doi.org/10.1016/j.bmc.2013.02.038>.
- Zhang, M.-R.; Haradahira, T.; Maeda, J.; Okauchi, T.; Kida, T.; Obayashi, S.; Suzuki, K.; Suhara, T. S. *J. Labelled Compd. Radiopharm.* **2002**, *45*, 857.
- Kikuchi, C.; Ando, T.; Watanabe, T.; Nagaso, H.; Okuno, M.; Hiranuma, T.; Koyama, M. *J. Med. Chem.* **2002**, *45*, 2197.
- Andriès, J.; Lemoine, L.; Mouchel-Blaisot, A.; Tang, S.; Verdurand, M.; Le Bars, D.; Zimmer, L.; Billard, T. *Bioorg. Med. Chem. Lett.* **2010**, *20*, 3730.
- Andriès, J.; Lemoine, L.; Le Bars, D.; Zimmer, L.; Billard, T. *Eur. J. Med. Chem.* **2011**, *46*, 3455.
- Lemonine, L.; Andriès, J.; Le Bars, D.; Billard, T.; Zimmer, L. *J. Nucl. Med.* **2011**, *52*, 1811.
- Lacivita, E.; Patarnello, D.; Stroth, N.; Caroli, A.; Niso, M.; Contino, M.; De Giorgio, P.; Di Pilato, P.; Colabufo, N. A.; Berardi, F.; Perrone, R.; Svenningsson, P.; Hedlund, P. B.; Leopoldo, M. *J. Med. Chem.* **2012**, *55*, 6375.
- Fukumura, T.; Suzuki, H.; Mukai, K.; Zhang, M.-R.; Yoshida, Y.; Nemoto, K.; Suzuki, K. *J. Labelled Compd. Radiopharm.* **2007**, *50*, S202.
- Zhang, M.-R.; Kida, T.; Noguchi, J.; Furutsuka, K.; Maeda, J.; Suhara, T.; Suzuki, K. *Nucl. Med. Biol.* **2003**, *30*, 513.
- Kumata, K.; Yui, J.; Hatori, A.; Fujinaga, M.; Yanamoto, K.; Yamasaki, T.; Kawamura, K.; Wakizaka, H.; Nengaki, N.; Yoshida, Y.; Ogawa, M.; Fukumura, T.; Zhang, M.-R. *J. Med. Chem.* **2011**, *54*, 6040.
- Fujinaga, M.; Yamasaki, T.; Kumata, K.; Kawamura, K.; Hatori, A.; Yanamoto, K.; Yui, J.; Yoshida, Y.; Ogawa, M.; Nengaki, N.; Maeda, J.; Fukumura, T.; Zhang, M.-R. *Bioorg. Med. Chem.* **2011**, *19*, 102.
- Maeda, J.; Suhara, T.; Ogawa, M.; Okauchi, T.; Kawabe, K.; Zhang, M.-R.; Semba, J.; Suzuki, K. *Synapse* **2001**, *40*, 122.
- Eckelman, W. C.; Mathis, C. A. *Nucl. Med. Biol.* **2006**, *33*, 161.
- Paterson, L. M.; Tyacke, R. J.; Nutt, D. J.; Knudsen, G. M. *J. Cereb. Blood Flow Metab.* **2010**, *30*, 1682.
- Khawaja, X.; Evans, N.; Reilly, Y.; Ennis, C.; Minchin, M. C. C. *J. Neuro. Chem.* **1995**, *64*, 2716.